Engineered Science

RESEARCH PAPER

View Article Online

Nano-mesoporous TiO_2 Vacancies Modification for Halide Perovskite Solar Cells

Qinglong Jiang,[1,2] Liang Wang,[3] Chao Yan,[4] Chuntai Liu,[5] Zhanhu Guo*[6] and Ning Wang*[1]

The efficiency of charge transport at interfaces and bulk affects the performance for lots optoelectronic devices. In this work, vacancies in nano-mesoporous TiO_2 have been modified by hydrogen peroxide and the corresponding photoactive electrode for halide perovskite solar cells shows remarkable improvement of current density (J_{sc}) 36% and open circuit voltage (V_{oc}) 10%, with overall improvement of efficiency over 75%. Photovoltage decay indicates the electron lifetime have been almost doubled after hydrogen peroxide treatment.

Keywords: Halide perovskite; solar cell; TiO_2; peroxide

Received 27th February 2018, Accepted 28th March 2018

DOI: 10.30919/es.180329

1. Introduction

In form of electrons or ions, charge transport at interfaces and in bulk phases plays a key role in the efficiency and performance for lots of optoelectronic devices, such as TiO_2 for solar cells,[1,2] electrolytes for electrochromic devices.[3,4] Halide perovskite materials have been find extensive applications in solar cell,[5,6] light emission devices,[7,8] detectors,[9] and lots of other fields.[10,11] With over 22% of efficiency over since it was first reported in 2009,[5,12] perovskite type $MPbX_3$ solar cells have attracted worldwide attention. One after another improvements achieved in the past few years suggest that it is the most promising candidate for the next generation solar cells.[12–14] Typically, perovskite solar cells are a sandwich structure: a meso-structured TiO_2 layer on FTO filled up with perovskite $CH_3NH_3PbX_3$ as active photoanode, doped spiro-MeOTAD as hole transport material layer (HTM) and a counter electrode (such as Au[15], Ag[16], Ni[17] or even carbon[18]).[19–21] As the electron transport layer, the morphology, thickness and crystallinity for both meso-structured TiO_2 layer and the compact TiO_2 electron-blocking layer,[22–24] play a crucial role in the efficiency of similar solar cells including dye sensitized solar cells.[23,25–27]

How efficient the charge can be separated and transported relate to the performance of solar cell.[2] The defects, especially the vacancies or dopants on the surface of TiO_2 mesoporous layer and block layer, affect the charge transport efficiency directly. As demonstrated in Figure 1, charge can be transferred more efficiently in the TiO_2 with no defects shown as trap free path. While in the case of TiO_2 with lots of oxygen vacancies ($\mathbf{V_o^{2+}}$) caused defects, charge can be trapped easily by these vacancies (path with traps) and caused recombination. In turn, the lifetime of electrons will be reduced and the charge transfer will be delayed causing severe recombination of electrons and holes at the defects.[10] As a result, the corresponding solar cell has lower J_{sc} and lower V_{oc}. In this work, the vacancies have been reduced by simply processing the nano-mesoporous TiO_2 in the H_2O_2.

The lifetime and charge transport can be measured by optical method,[28] and usually the results are not on the real solar cell. The photovoltage transient measurements are the direct measurement of voltage change under light vs. time,[17,23,29] which reflect the actual situation in real solar cells. In this study, the life time of photo-charge processes are studied by photovoltage transient measurements. The halide perovskite solar cells based on vacancies removed TiO_2 shows 20.2 mA/cm^2 J_{sc} and 0.82 V of V_{oc}, which are 36% and 10% higher than the halide perovskite solar cells based on the TiO_2 with vacancies.

2. Experimental section

2.1. TiO_2 blocking layer on FTO slide

1 cm ×2 cm FTO glass slides were washed and ultrasonicated in distilled deionized water, isopropanol, acetone and ethanol sequentially.

[1] *State Key Laboratory of Marine Resource Utilization in South China Sea, Hainan University, Haikou, P. R. China. E-mail: wangn02@foxmail.com*
[2] *Materials Science Division, Argonne National Laboratory, Lemont, IL, USA*
[3] *College of Chemistry and Pharmaceutical Sciences, Qingdao Agricultural University, Qingdao 266109, China*
[4] *School of Material Science and Engineering, Jiangsu University of Science and Technology, No 2, Mengxi Rd, Zhenjiang, Jiangsu, China*
[5] *School of Materials Science and Engineering, The Key Laboratory of Material Processing and Mold of Ministry of Education, Zhengzhou University, Zhengzhou, China*
[6] *Department of Chemical and Biomolecular Engineering, University of Tennessee, Knoxville, TN, USA. E-mail: zguo10@utk.edu*

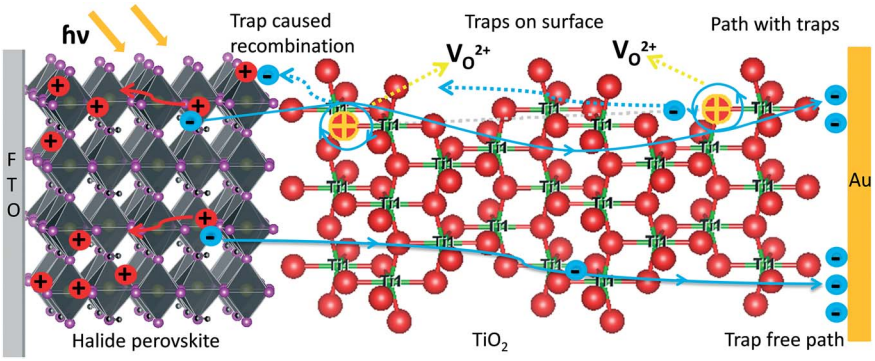

Fig. 1 Illustration of Oxygen vacancies (V_O^{2+}) caused defects indicate charge can be trapped and cause the delay of charge transfer.

Distilled deionized water was used to rinse the substrates between each step. Before use, the washed FTO glass slides were further cleaned with oxygen plasma for 15 mins. The FTO slides were heat up to 450 °C on a hot plate and 0.2 M Ti(IV) bis(ethyl acetoacetate)-diisopropoxide in 1-butanol solution was sprayed, followed by annealing at 450 °C for 1 h in air.

2.2. Nano-mesoporous TiO_2 on FTO slide

12 ml Titanium isopropoxide ($Ti(O^iPr)_4$, Aldrich, 97%) and 3 ml propanediol were added dropwise into 80 ml water and 25 ml acetic acid at 0 °C. The mixture was heated to 78 °C over 1 h with stirring and kept at this temperature for another 3.5 hrs. The prepared colloidal solution was concentrated to 100 ml by rotary evaporation, followed by loading into a Teflon insert titanium autoclave and heated to 200 °C over 1 h and held for 12 hrs. The resulting mixture (8 g), terpineol (1 ml) and methylcellulose (0.25 g) were mixed under stirring for 4 hrs. The prepared TiO_2 paste was spread on FTO glass slide by doctor blade, followed by heat treatment at 550 °C for 2 hrs.

2.3. Remove of defects by hydrogen peroxide.

The nano-mesoporous TiO_2-FTO glass slides were dipped in a H_2O_2 (30 wt%) /NH_4OH (25 wt%) (10:1 of volume ratio) solution for 5 min. After annealing at 450 °C for 30 min under O_2 atmosphere, the synthesize TiO_2-FTO glass slides were further soaked in 40 mM $TiCl_4$ solution at 70 °C for 1 h and rinsed with DI water. Finally, the $TiCl_4$ treated TiO_2-FTO glass slides were annealed at 500 °C for 30 minutes.

2.4. CH_3NH_3I and perovskite $CH_3NH_3PbI_3$ precursory

Aqueous methylamine (19.5 ml, 40 wt % solution, Aldrich) was added to hydroiodic acid (32.3 ml, 57 wt % aqueous solution, Aldrich) in an ice bath slowly with stirring for 2 hrs. The liquid mixture was extracted by rotary evaporator at 50 °C to get rid of most of the solvent. The product with brownish color was filtered and washed by diethyl ether until turn into white. The white product was recrystallized in ethanol and diethyl ether. PbI_2 (0.30 g, Aldrich) and CH_3NH_3I (0.10 g) were dissolved in γ-butyrolactone (0.5 ml, Aldrich) at 80 °C to produce perovskite precursor solution.

2.5. Hole transport material (HTM)

Spiro-MeOTAD (92 mg, 2,2',7,7'-tetrakis(N,N-di-p-methoxyphenylamine)-9,9'- spiro-bifluorene), Lithium bis-trifluoromethane sulfonamide (7.2 mg) and 4-tert-butylpyridine (12 mg, TBP) were dissolved in chlorobenzene (1 ml).

2.6. Halide perovskites solar cell

$CH_3NH_3PbI_3$ perovskite precursor was spin coated on nano-mesoporous TiO_2-FTO slide with 2000 rmp for 1 min in air (R.H. <30%), and annealed in air for 10 minutes at 105 °C. HTM was spin coated at 2500 rpm. Au film (80 nm) was thermal coated on as counter electrode.

2.6 Characterization

The current density-voltage (*J-V*) curves were collected on Potentiostat (CHI 600) and solar simulator (Photo Emission Inc. CA) at 200 mV/s. The open-circuit photovoltage transient was measured at a resolution of 10 μs per data point with an ultrafast optical shutter to control the incident sunlight (UniBlitz, 0.7 ms response time). In order to verify that there is no limitation in the measurement for our setup, a silicon photodiode (OSRAM Opto Semiconductor, 20 ns response time, 400 nm-1100 nm) is used as a reference. XRD was taken on X-ray powder diffractmeter (X'Pert PRO, PANalytical, Almelo, The Netherlands).

3. Results and discussion

3.1. Characterization of TiO_2 on FTO glass slide and J-V curves

Figure 2a shows the X-ray diffraction (XRD) patterns of TiO_2-FTO glass slide for both H_2O_2 treated and untreated reference. Peaks from FTO glass are indicated by triangles. No XRD patterns change can be observed including peaks disappear, new peaks appear and peak shifts. XRD patterns indicate H_2O_2 treatment will not affect the crystal structure of TiO_2.

Figure 2b is the comparison of J-V curves for the H_2O_2 treated and untreated TiO_2 based halide perovskite solar cells. The insets in Figure 2b are the SEM images of the cross section for both the processed and reference halide perovskite solar cell, which indicating about 80 nm of Au counter electrode, 200 nm HTM layer and 400 nm halide perovskite/TiO_2. Halide perovskite solar cell based on H_2O_2 processed TiO_2 as working electrode outperformed the solar cell based on reference TiO_2 as working electrode. Table 1 summarizes the parameters of J_{sc}, V_{oc}, fill factor (FF) and the efficiency (η).

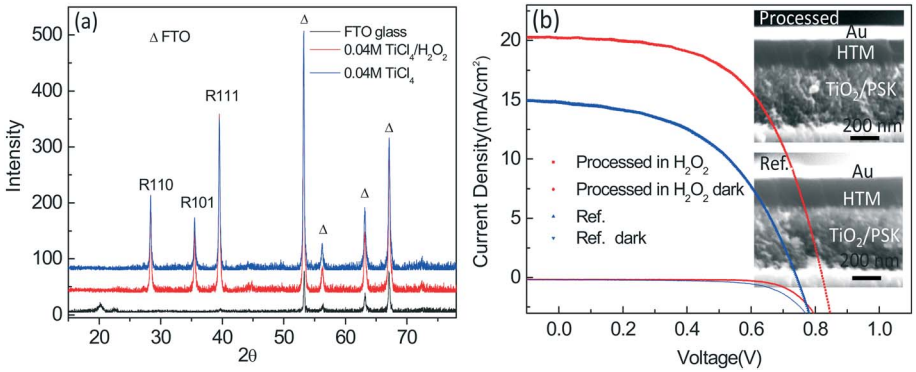

Fig. 2 a: XRD patterns of TiO_2 on FTO substrate; b: comparison of J-V curves of halide perovskite solar cells with and without H_2O_2 processed TiO_2 as photon anode.

Apparently, solar cell based on H_2O_2 processed nano-mesoporous TiO_2 exhibits high current density 20.2 mA/cm^2, which is 9.2% higher comparing with 14.8 mA/cm^2 for the reference solar cell. The V_{oc} is 0.82 V for the H_2O_2 processed nano-mesoporous TiO_2 based solar cell with an improvement of 10.8% (0.74 V for reference solar cell). Also, H_2O_2 processed nano-mesoporous TiO_2 based solar cell has higher Shunt resistance (R_{sh}) and lower series resistance (R_s). Overall, the improvement of efficiency is 75.9% for the H_2O_2 processed TiO_2 based solar cell (9.44%) comparing with untreated solar cell (5.37%).

3.2. Photovoltage transient measurements

Electron lifetime can be measured by optical method and photovoltage transient. The electron lifetime measured by photovoltage transient is based on actual solar cell which combines the effects of both electrons and holes, the interface contact and even the thermal effect from the light. Figure 3a shows the photovoltage transient curves for the H_2O_2 processed nano-mesoporous TiO_2 based solar cell and untreated TiO_2 based perovskite solar cells. The setup for the photovoltage transient test has been approved in the previous reports.[17,23]

Figure 3b shows the photovoltage rising transient time (90% of the maximum V_{oc}) time of V_{oc} which are 0.1608 s and 0.2218 s for the halide perovskite solar cell based on H_2O_2 treated nano-mesoporous TiO_2 and solar cells based on untreated TiO_2 as photoactive electrodes, respectively. H_2O_2 treatment for TiO_2 obviously improved the V_{oc} and reduce the photovoltage rising time for perovskite solar cell. In order to assure a fast open can close of aperture for the light, the size of the light spot on the solar cell is smaller than the light spot for the J-V test resulting in a lower voltage.

3.3. Analysis of photovoltage transient decay

The electron lifetimes (τ_e) for halide perovskite solar cell based on H_2O_2 treated and untreated TiO_2 have been calculated by photovoltage transients decay according to equation:[30,31]

$$\tau_e = \frac{k_B T}{e}\left(\frac{dV_{oc}}{dt}\right)^{-1}$$

where k_B is the Boltzmann constant, T is the absolute temperature in K, e is the charge of an electron, and dV_{oc}/d_t is the derivative of the open-circuit photovoltage transient.

Figure 4a is the photovoltage decay curve. The corresponding electron lifetimes as a function of open-circuit photovoltage extracted from the open-circuit photovoltage decay data are presented in Figure 4b. Halide perovskite solar cell based on H_2O_2 treated nano-mesoporous TiO_2 has a slower decay rate, which indicating a longer electron lifetime, less charge recombination and higher charge collection efficiency. The electron lifetime for untreated reference solar cell is about half for the H_2O_2 treated TiO_2 based solar cell, which lead to large electron recombination and negatively affects V_{oc}, J_{sc} and FF.[31]

4. Conclusions

In conclusion, a simple and easy hydrogen peroxide treatment has been used to reduce the oxygen vacancies caused defects in TiO_2. The corresponding perovskite solar cell based on the H_2O_2 processed nano-mesoporous TiO_2 indicates significant improvement in J_{sc}, V_{oc} and thus the overall PCE improves from 5.4% for the reference solar cell to 9.5%.

5. Conflict of interest

The authors declare no competing financial interests.

Table 1 Comparison of photovoltaic performance for solar cells with and without processed nano-mesoporous TiO_2 by H_2O_2 as photoanodes.

TiO_2	J_{sc} (mA/cm^2)	V_{oc} (V)	FF	η (%)	R_{sh} (Ω)	R_s (Ω)
H_2O_2 processed	20.22	0.82	0.57	9.44	433.91	11.0
Reference	14.81	0.74	0.49	5.37	127.12	96.52

Note: R_{sh}= Shunt resistance, R_s=series resistance

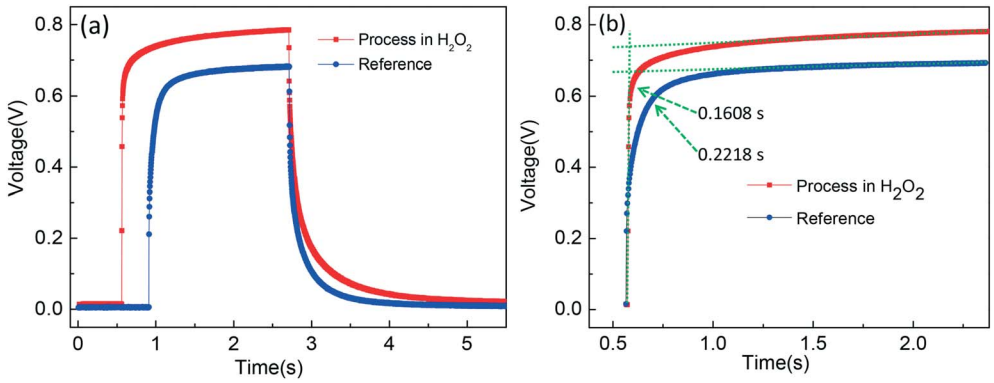

Fig. 3 Pulse white light incident caused photovoltage transient of perovskite solar cell based on nano-mesoporous TiO_2 with and without H_2O_2 treatment. a: rising and decay transient; b: Comparison of photovoltage rising transient.

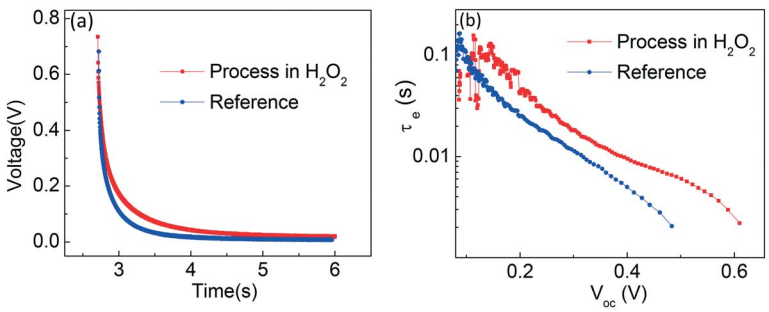

Fig. 4 (a) Photovoltage decay and (b) electron lifetimes (τ_e) for perovskite solar cells based on H_2O_2 treated and untreated TiO_2.

Acknowledgments

We are grateful to NSFC (21776148) and the Natural Science Foundation of Shandong Province (ZR2016BM07). Financial supports from the Qingdao Special Research Foundation of Science and Technology (16-6-2-29-nsh) are also gratefully acknowledged.

References

1 C. C. Mercado, F. J. Knorr and J. L. McHale, *ACS Nano*, 2012, **6**, 7270–7280.
2 X. Feng, K. Zhu, A. J. Frank, C. A. Grimes and T. E. Mallouk, *Angew. Chem. Int. Ed. Engl.*, 2012, **51**, 2727–2730.
3 X. Tu, X. Fu and Q. Jiang, *Displays*, 2010, **31**, 150–154.
4 Y.-F. Gong, X.-K. Fu, S.-P. Zhang and Q.-L. Jiang, *Chinese J. Chem.*, 2007, **25**, 1743–1747.
5 A. Kojima, K. Teshima, Y. Shirai and T. Miyasaka, *J. Am. Chem. Soc.*, 2009, **131**, 6050–6051.
6 Q. Jiang and T. Xu, *Comments Inorg. Chem.*, 2015, **36**, 200–214.
7 J. Li, X. Shan, S. G. Bade, T. Geske, Q. Jiang, X. Yang and Z. Yu, *J. Phys. Chem. Lett.*, 2016, 4059–4066.
8 Q. Jiang, M. Chen, J. Li, M. Wang, X. Zeng, T. Besara, J. Lu, Y. Xin, X. Shan, B. Pan, C. Wang, S. Lin, T. Siegrist, Q. Xiao and Z. Yu, *ACS Nano*, 2017, **11**, 1073–1079.
9 S. Yakunin, M. Sytnyk, D. Kriegner, S. Shrestha, M. Richter, G. J. Matt, H. Azimi, C. J. Brabec, J. Stangl, M. V. Kovalenko and W. Heiss, *Nat. Photonics*, 2015, **9**, 444–449.
10 Q. Jiang, X. Zeng, N. Wang, Z. Xiao, Z. Guo and J. Lu, *ACS Energy Lett.*, 2018, **3**, 264–269.
11 J. A. Dawson, A. J. Naylor, C. Eames, M. Roberts, W. Zhang, H. J. Snaith, P. G. Bruce and M. S. Islam, *ACS Energy Lett.*, 2017, **2**, 1818–1824.
12 W. S. Yang, B. W. Park, E. H. Jung, N. J. Jeon, Y. C. Kim, D. U. Lee, S. S. Shin, J. Seo, E. K. Kim, J. H. Noh and S. I. Seok, *Science*, 2017, **356**, 1376–1379.
13 Y. Guo, T. Liu, N. Wang, Q. Luo, H. Lin, J. Li and Q. Jiang, L. Wu and Z. Guo, *Nano Energy*, 2017, **38**, 193–200.
14 S. Kazim, M. K. Nazeeruddin, M. Gratzel and S. Ahmad, *Angew. Chem. Int. Ed. Engl.*, 2014, **53**, 2812–2824.
15 J. Burschka, N. Pellet, S. J. Moon, R. Humphry-Baker, P. Gao, M. K. Nazeeruddin and M. Gratzel, *Nature*, 2013, **499**, 316–320.
16 M. Liu, M. B. Johnston and H. J. Snaith, *Nature*, 2013, **501**, 395–398.
17 Q. Jiang, X. Sheng, B. Shi, X. Feng and T. Xu, *J. Phys. Chem. C*, 2014, **118**, 25878–25883.
18 A. Mei, X. Li, L. Liu, Z. Ku, T. Liu, Y. Rong, M. Xu, M. Hu, J. Chen, Y. Yang, M. Gratzel and H. Han, *Science*, 2014, **345**, 295–298.
19 I. C. Smith, E. T. Hoke, D. Solis-Ibarra, M. D. McGehee and H. I. Karunadasa, *Angew. Chem. Int. Ed. Engl.*, 2014.
20 N. Marinova, W. Tress, R. Humphry-Baker, M. I. Dar, V. Bojinov, S. M. Zakeeruddin, M. K. Nazeeruddin and M. Gratzel, *ACS Nano*, 2015, **9**, 4200–4209.

21 T. Xu, L. Chen, Z. Guo and T. Ma, *Phys. Chem. Chem. Phys.*, 2016, **18**, 27026–27050.
22 M. M. Lee, J. Teuscher, T. Miyasaka, T. N. Murakami and H. J. Snaith, *Science*, 2012, **338**, 643–647.
23 Q. Jiang, X. Sheng, Y. Li, X. Feng and T. Xu, *Chem Commun.*, 2014, **50**, 14720–14723.
24 L. Liu, J. Qian, B. Li, Y. Cui, X. Zhou, X. Guo and W. Ding, *Chem Commun.*, 2010, **46**, 2402–2404.
25 A. Yella, L. P. Heiniger, P. Gao, M. K. Nazeeruddin and M. Gratzel, *Nano Lett.*, 2014, **14**, 2591–2596.
26 Y. Rong, Z. Ku, A. Mei, T. Liu, M. Xu, S. Ko, X. Li and H. Han, *J. Phys. Chem. Lett.*, 2014, **5**, 2160–2164.
27 Q. Jiang, Y.-P. Yeh, N. Lu, H.-W. Kuo, M. Lesslie and T. Xu, *J. Renew. Sustain. Ener*, 2016, **8**, 013701.
28 S. D. Stranks, G. E. Eperon, G. Grancini, C. Menelaou, M. J. Alcocer, T. Leijtens, L. M. Herz, A. Petrozza and H. J. Snaith, *Science*, 2013, **342**, 341–344.
29 B. C. O'Regan, K. Bakker, J. Kroeze, H. Smit, P. Sommeling and J. R. Durrant, *J. Phys. Chem. B*, 2006, **110**, 17155–17160.
30 Y. Bai, H. Yu, Z. Zhu, K. Jiang, T. Zhang, N. Zhao, S. Yang and H. Yan, *J. Mater. Chem. A*, 2015, **3**, 9098–9102.
31 K. T. Dembele, G. S. Selopal, R. Milan, C. Trudeau, D. Benetti, A. Soudi, M. M. Natile, G. Sberveglieri, S. Cloutier, I. Concina, F. Rosei and A. Vomiero, *J. Mater. Chem. A*, 2015, **3**, 2580–2588.

